Analytical Biochemistry 407 (2010) 211–219

Contents lists available at ScienceDirect

Analytical Biochemistry

journal homepage: www.elsevier.com/locate/yabio

Site-specific conjugation of metal carbonyl dendrimer to antibody and its use as detection reagent in immunoassay

Nathalie Fischer-Durand [a], Michèle Salmain [a], Bogna Rudolf [b], Lili Dai [a], Lauriane Jugé [c], Vincent Guérineau [d], Olivier Laprévote [d], Anne Vessières [a,*], Gérard Jaouen [a]

[a] Chimie ParisTech (Ecole Nationale Supérieure de Chimie de Paris), Laboratoire Charles Friedel, CNRS UMR 7223, 75005 Paris, France
[b] Department of Organic Chemistry, University of Lodz, 91-403 Lodz, Poland
[c] Chimie ParisTech, Service de RMN, 75231 Paris Cedex 05, France
[d] Centre de recherche de Gif, Institut de Chimie des Substances Naturelles, CNRS, 91198 Gif sur Yvette Cedex, France

ARTICLE INFO

Article history:
Received 9 June 2010
Received in revised form 28 July 2010
Accepted 20 August 2010
Available online 15 September 2010

Keywords:
Antibody labeling
Dendrimers
Carbonyl ligands
Immunochemistry
IR spectroscopy

ABSTRACT

We describe here the conjugation of polyclonal goat anti-rabbit antibody to generation 4 polyamidoamine (G4–PAMAM) dendrimers carrying (i) (η^5-cyclopentadienyl) iron dicarbonyl succinimidato complexes as infrared (IR) probes, (ii) nitroaniline entities as nuclear magnetic resonance (NMR) probes, (iii) acetamide groups for surface neutralization, and (iv) hydrazide-terminated spacer arms for the reaction with aldehyde. To preserve a high binding affinity, the conjugation was performed on the carbohydrate moieties located on the Fc fragment. The resulting conjugates were characterized by Fourier transform–IR, ultraviolet (UV), and high-mass matrix-assisted laser desorption/ionization time-of-flight (MALDI–TOF) mass spectrometry. On the basis of relative concentration ratios of IR probes and antibody, an average labeling of 30 IR probes per antibody was reached (i.e., more than twice the value obtained with our previous strategy that generated no spacer arm). Immunoassays revealed that the antibody–dendrimer conjugates retained 55.1% of immunoreactivity on average with respect to underivatized antibody. Finally, the conjugates were used to quantify their antigen by solid-phase carbonyl metallo immunoassay (CMIA). Results showed a significant enhancement of the IR signal, demonstrating the efficiency of the new conjugation strategy and the potential of the new antibody–dendrimer conjugates as universal immunoanalytical reagents.

Dendrimers, and particularly polyaminoamine (PAMAM)[1] dendrimers [1–4], are playing an increasing role in the field of bioconjugation. This growing interest is attested by the number of articles and reviews devoted to this subject and is illustrated by a specific chapter titled "Dendrimers and Dendrons," including their mode of conjugation, in the 2008 second edition of the well-known book Bioconjugate Techniques [5]. Their popularity in the field is due to their water solubility, their lack of immunogenicity, their availability in a variety of sizes (termed generations), and their versatile surface functionalities. These properties make dendrimers ideal platforms for the construction of complex protein conjugates for a wide range of applications, including drug delivery [6–18] diagnosis [19–23], biosensing interfaces for the design of biosensors [24–29], and signal enhancement in immunoassays [30–32]. Some of these applications involved the conjugation between engineered dendrimers and antibodies so as to introduce a high number of active compounds on the antibody molecule or immunoglobulin G (IgG) so as to improve a given effect (e.g., fluorescence signal, delivery of therapeutics). Most of the previously reported conjugation strategies involved the use of heterobifunctional cross-linkers such as sulfosuccinimidyl-4-(*N*-maleimidomethyl)cyclohexane-1-carboxylate (sulfo-SMCC) and *N*-succinimidyl-3-(2-pyridyldithio)propionate (SPDP) to introduce maleimide [23,33–38] and thiol [39,40] groups on the IgG molecule. These conjugation procedures involve amine groups that are located uniformly on the surface of the immunoglobulin, thereby leading to random addition of the cross-linker and to potential blocking of the antigen binding site. On the contrary, one of the possible site-selective conjugation strategies takes advantage of the carbohydrate chains located in the Fc region, thereby preserving the remote antigen binding sites. Mild oxidation of the carbohydrate moieties generates aldehyde groups allowing conjugation reactions with amines or hydrazides. Only a

* Corresponding author. Fax: +33 1 43 26 00 61.
E-mail address: a-vessieres@chimie-paristech.fr (A. Vessières).

[1] *Abbreviations used*: PAMAM, polyaminoamine; IgG, immunoglobulin G; sulfo-SMCC, sulfosuccinimidyl-4-(N-maleimidomethyl) cyclohexane-1-carboxylate; SPDP, N-succinimidyl-3-(2-pyridyldithio) propionate; CMIA, carbonyl metallo immunoassay; IR, infrared; G4, generation 4; NMR, nuclear magnetic resonance; FT, Fourier transform; UV, ultraviolet; MALDI–TOF, matrix-assisted laser desorption/ionization time-of-flight; DIPEA, N,N-diisopropylethylamine; TSTU, N,N,N',N'-tetramethyl-O-(N-succinimidyl) uronium tetrafluoroborate; Vis, visible; NaPB, sodium phosphate buffer; MeOH, methanol; SA, sinapic acid; DMF, dimethylformamide; PBS, phosphate-buffered saline; HRP, horseradish peroxidase; β-LG, β-lactoglobulin.

0003-2697/$ - see front matter © 2010 Elsevier Inc. All rights reserved.
doi:10.1016/j.ab.2010.08.027

few authors reported the linkage of dendrimers to antibodies using this site-directed chemical reaction [41–44]. Whatever the conjugation strategy, coupling ratios of approximately 1 dendrimer per IgG were reported.

We are currently involved in the labeling of antibodies with transition metal carbonyl complexes using amine-terminated PAMAM dendrimers as label carriers. These antibody–dendrimer metal carbonyl complexes are intended to be used as new universal detection reagents in a modified solid-phase format of the carbonyl metallo immunoassay (CMIA) that we introduced during the early 1990s [45–49]. CMIA takes advantage of the unique signals generated by transition metal carbonyl complexes that display intense vibration bands (ν_{CO}) in the mid-infrared (IR) spectral range (1800–2200 cm^{-1}) where few other molecules absorb, thereby allowing their quantification by measuring the height of the ν_{CO} bands, which is proportional to the quantity of complex. As a consequence, the more metal carbonyl complexes (IR probes) are linked to the antibody, the higher the resulting IR signal is. In this regard, PAMAM dendrimers are ideal carriers to covalently couple multiple IR probes to antibodies. We previously described the site-directed conjugation of PAMAM–$(NH_2)_{64}$ or generation 4 (G4)–PAMAM carrying 10 to 25 (η^5-cyclopentadienyl) iron dicarbonyl succinimidato (Fp) units to oxidized goat anti-rabbit IgG through reductive amination using the remaining surface amines of the dendrimer [44]. This strategy afforded immunoconjugates with a loading of metal carbonyl dendrimer highly dependent on the steric hindrance around the free amino groups on the surface of the dendrimer. We showed that the dendrimer carrying 10 Fp complexes led to the attachment of 1.4 dendrimers per IgG, whereas the dendrimer carrying 25 Fp complexes led to the attachment of only 0.5 dendrimer per IgG. In other words, we were able to bind 13 Fp units per IgG on average. To further enhance the labeling of antibodies with Fp complexes, thereby affording a larger amplification of the IR signal, and to fully exploit the 64 potential conjugation sites of G4–PAMAM, we then designed a more advanced generation of PAMAM dendrimers carrying 20 to 30 Fp complexes and a functionalized spacer arm [50] intended to move the dendrimer away from the IgG so as to decrease the steric hindrance between the two macromolecules. The spacer encompassed a nitroaromatic entity whose aromatic protons served as nuclear magnetic resonance (NMR) probe to estimate the average number of substituents conjugated at each functionalization step (as a consequence, all of the coupling ratios reported here correspond to average, and not absolute, values). It was terminated by a hydrazide function known to react with aldehydes at slightly acidic pH, thereby avoiding self-condensation of oxidized IgG with amine residues that may occur at neutral or basic pH.

In the current article, we describe the conjugation of oxidized goat anti-rabbit IgG to our new hydrazide-based Fp-labeled G4–PAMAM dendrimers whose improved synthetic route is also reported. The new immunoconjugates were analyzed by Fourier transform (FT)–IR, ultraviolet (UV), and high-mass matrix-assisted laser desorption/ionization time-of-flight (MALDI–TOF) mass spectrometry to evaluate the efficiency of the new dendrimer design on the coupling ratio. Immunoreactivity studies were then conducted for the first time on these antibody–metallodendrimer conjugates to assess the influence of the dendrimer loading and the coupling ratio on their affinity for rabbit IgG. Finally, they were involved in the quantification of rabbit IgG by solid-phase CMIA to assess the efficiency of the new bioconjugation strategy on the intensity of the IR signal.

Materials and methods

Materials

Amine-terminated G4–PAMAM dendrimer ethylenediamine core, 4-fluoro-3-nitrobenzoic acid, *N,N*-diisopropylethylamine (DIPEA), acetic anhydride, 1,1,1-trifluoroethanol, and *N,N,N',N'*-tetramethyl-*O*-(*N*-succinimidyl)uronium tetrafluoroborate (TSTU) were purchased from Sigma–Aldrich. Fp–maleimide was synthesized as described previously [51]. Dialysis was performed with Spectra/Por 1 membranes with a molecular weight cutoff of 6000 to 8000 Da (Spectrum Laboratories). Nitrocellulose membranes (pore size 0.45 μm) were purchased from Bio-Rad (product no. 162-0117). Flash chromatography was performed on silica gel 60 (40–63 μm, Merck). Gel filtration column Superdex 200 HiLoad 16/60 and 5-ml HiTrap desalting column were purchased from GE Healthcare. UV/visible (Vis) spectra were recorded on a UV/mc^2 spectrometer (Safas, Monaco). NMR spectra were recorded on Bruker Avance 300 and Avance 400 spectrometers. Sodium phosphate buffer (NaPB) was a 10 mM NaPB (pH 7.2) containing 0.2 M NaH_2PO_4 (11 ml) and 0.2 M Na_2HPO_4 (39 ml) diluted to 1 L of deionized water with 0.15 M NaCl. Citrate buffer (pH 6.0) was 10 mM citrate buffer containing 130 mM NaCl.

FT–IR spectroscopy

FT–IR spectra were recorded on a benchtop Bruker Tensor 27 IR spectrometer equipped with a DTGS (deuterated triglycine sulfate) detector and a 6-mm-diameter membrane holder perpendicularly positioned with respect to the IR beam. FT–IR data were recorded and manipulated on a Windows-operating PC using OPUS 6.5 software. Routinely, 44 scans were co-added in 40 s, and the resulting interferogram was apodized using a Blackman–Harris three-term function and then Fourier-transformed to yield a 4-cm^{-1} resolution spectrum.

The calibration curve used for the quantification of the metallodendrimers and the immunoconjugates was established as follows. Standard solutions of Fp–maleimide in the range of 50 to 660 nmol/ml in 10 mM NaPB (pH 7.2) were spotted (4 μl) onto punched nitrocellulose membranes (diameter = 6 mm). A blank was made by spotting 4 μl of NaPB. Membranes were dried for at least 2 h at room temperature before IR recording in the range of 1800 to 2200 cm^{-1}. The calibration curve was constructed by plotting the absorbance at 2052 cm^{-1} versus the concentration of the standard solutions of Fp–maleimide. This experiment was repeated several times and gave reproducible standard straight lines.

Quantification of Fp entities in the metallodendrimer solutions was carried out as follows. The conjugate was dissolved in 2 ml of methanol (MeOH) and then diluted appropriately with 10 mM NaPB (pH 7.2). Then 4 μl in duplicate was spotted onto nitrocellulose membranes and dried. A blank membrane was prepared by spotting 4 μl of NaPB. In the case of antibody–dendrimer conjugate samples, the final solution after purification and concentration was diluted 4 times in 10 mM NaPB (pH 7.2). FT–IR spectra were then recorded between 1800 and 2200 cm^{-1}. Absorbances at 2052 cm^{-1} were used to calculate the average concentration of Fp entities using the calibration curve established above.

MALDI–TOF mass spectrometry

A Voyager DE-STR MALDI–TOF mass spectrometer (Perseptive Biosystems, Framingham, MA, USA), equipped with a 337-nm pulsed nitrogen laser (20 Hz) and an Acqiris 2-GHz digitizer board, was used for all experiments.

The detection was done with a dedicated high-mass detection system (HM1, CovalX, Zurich, Switzerland). This system, which is based on unique conversion dynode technology, enhances sensitivity in the high-mass range up to 100 kDa and avoids detector saturation due to intense low-mass (e.g., matrix) species [52]. The low saturation is critical to ensure detection over a broad dynamic range.

Mass spectra were obtained in linear positive ion mode with the following settings: accelerating voltage of 25 kV, grid voltage 93% of accelerating voltage, and extraction delay time of 700 ns. The laser intensity was set just above the ion generation threshold to obtain peaks with the highest possible signal-to-noise ratio without significant peak broadening.

The mass spectrometer was externally calibrated using the protonated monomer and dimer of IgG. All data were processed using the Data Explorer software package (Applied Biosystems).

Sinapic acid (SA) was used as the matrix. The SA matrix solution was prepared by dissolving 10 mg in 500 μl of water and 500 μl of acetonitrile. Antibody–dendrimer conjugates were extensively dialyzed in 20 mM ammonium acetate before analysis. Then 1 μl of the analyte and 9 μl of the matrix solution were mixed together, and 1 μl of the resulting solution was spotted on the MALDI plate and air-dried (“dried droplet” method).

Precautions for handling dendrimers

The functionalized dendrimers described in this article must be kept in solution at all times otherwise it is not possible to dissolve them again. Consequently, compounds cannot be thoroughly dried before NMR recording. Accordingly, to eliminate MeOH traces, each sample is evaporated to dryness for no longer than 1 min and then is dissolved two times with 0.8 ml of MeOH-d_4 and evaporated. Because functionalized dendrimers were not unimolecular, their characterization by NMR represented the average value of their polymeric distribution.

Synthesis of hydrazine carboxylic acid, 2-[6-(4-fluoro-3-nitrobenzoyl)amino-1-oxohexyl]-1-tert-butyl ester (1)

DIPEA (98.5 μl, 0.56 mmol) and TSTU (136 mg, 0.45 mmol) were added to a solution of 4-fluoro-3-nitrobenzoic acid (69.8 mg, 0.377 mmol) in dimethylformamide (DMF, 2 ml). The solution was stirred at room temperature for 45 min, and then hydrazine carboxylic acid [2-(6-amino-1-oxohexyl)-1-*tert*-butyl ester] prepared previously [50] (92.4 mg, 0.377 mmol) in DMF (1 ml) was added dropwise and the reaction mixture was stirred at room temperature for 7 h. EtOAc (15 ml) and a saturated aqueous solution of $NaHCO_3$ (15 ml) were added, and the aqueous layer was extracted with EtOAc (3 × 15 ml). Organic layers were combined and washed with water (2 × 20 ml) and then dried (Na_2SO_4). The crude compound was purified by flash chromatography on silica gel (EtOAc, R_f = 0.35) to afford compound **1** as a pale yellow oil (50 mg, 30% yield): ^{1}H NMR (300 MHz, $CDCl_3$) δ 1.33 (s, 9 H), 1.38 (m, 2 H), 1.53–1.68 (m, 4 H), 2.20 (t, J = 7.20 Hz, 2 H), 3.38 (q, J = 6.0 Hz, 2 H), 6.79 (s, NH), 7.28 (dd, J_{HF} = 10.3 Hz, J_{HH} = 8.8 Hz, H_{5Ar}), 8.16 (ddd, J_{HH} = 2.2 Hz, J_{HF} = 4.2 Hz, J_{HH} = 8.6 Hz, H_{6Ar}), 8.55 (dd, J_{HF} = 7.0 Hz, J_{HH} = 2.2 Hz, H_{2Ar}); ^{13}C NMR (75.5 MHz, $CDCl_3$) δ 24.21, 25.95, 28.05, 28.41, 33.42, 39.87, 81.82, 118.65 (d, J_{CF} = 21.1 Hz), 125.10, 131.51, 134.90 (d, J_{CF} = 9.1 Hz), 136.96 (d, J_{CF} = 8.0 Hz), 155.75, 156.95 (d, J_{CF} = 269.3 Hz), m/z (CI/NH_3) 430 (40%, $[M+NH_4]^+$), 413 (25%, $[M+H]^+$), 374 (10), 357 (15), 330 (20), 313 (100); HRMS (CI/CH_4) m/z calculated for $C_{18}H_{26}O_6N_4F$ $(M+H)^+$ 413.1836, observed 413.1853.

Synthesis of PAMAM–G4(ArHydrNHBoc)$_x$Fp$_y$

Compound **1** (5 equiv) and DIPEA (10 equiv) were added to a solution of G4–PAMAM in MeOH and stirred at room temperature for 48 h. The resulting conjugate was purified by dialysis in MeOH and analyzed by ^{1}H NMR (see “Precautions for handling dendrimers” section above) to estimate the average number of aromatic residues covalently linked to the dendrimer amino groups through comparative peak integration of one of the aromatic protons at 8.7, 8.0, or 7.17 ppm versus the 744 protons of G4–PAMAM at 2.40, 2.61, and 2.82 ppm. The dendrimer was then allowed to react with Fp–maleimide (40 equiv) in MeOH at room temperature in the dark for 3 to 4 days and was purified by dialysis in MeOH. The resulting conjugate was analyzed (i) by ^{1}H NMR to assess the average number of Fp labels attached per dendrimer, (ii) by FT–IR spectroscopy to quantify the concentration of Fp entities according to the procedure described in the “FT–IR spectroscopy” section above, leading to the concentration of the dendrimer based on the coupling ratio estimated by ^{1}H NMR spectroscopy (80% yield from commercial G4–PAMAM).

Synthesis of PAMAM–G4(ArHydrNHBoc)$_x$Fp$_y$NHAc$_z$

This procedure was described in our previous report [50].

Removal of the t-Boc protective group

The reaction was performed as described previously [50], but a different workup was applied; at the end of the reaction time, the reaction mixture was diluted with H_2O (280 μl) and the pH was adjusted to approximately 6.0 with DIPEA (130 μl) to yield a clear orange solution. This solution was dialyzed in 50 mM AcONa + 150 mM NaCl (pH 5.0) for 18 h and purified on a gel filtration column (Superdex 200 HiLoad 16/60) [50]. A calibration curve at 280 nm was established by plotting A_{280} versus standard concentrations of this dendrimer solution in the range of 0.312 to 20 nmol/ml for further characterization of the antibody–dendrimer conjugates.

Preparation of antibody–dendrimer conjugates

$NaIO_4$ (0.1 M) in citric acid solution (10 mM, 24.7 μl) was added to a solution of goat anti-rabbit IgG (2 mg) in NaPB (142.4 μl), and the pH was adjusted to 3.7 with citric acid solution (10 mM, 80 μl). This solution was incubated for 1 h at room temperature in the dark and then quickly purified on a 5-ml HiTrap fast desalting column (50 mM AcONa + 150 mM NaCl, pH 5.0). Oxidized IgG solution was concentrated and transferred into 0.1 M AcONa (pH 5.1) and allowed to react with the PAMAM–G4(ArHydrNH_2)$_x$Fp$_y$NHAc$_z$ conjugate (8 mol equiv) at room temperature in the dark for 18 h. $NaBH_3CN$ (2.5 M in H_2O, 32 μl, final concentration = 100 mM) was added, and the incubation was pursued for 2.5 h before ethanolamine–HCl (1 M in H_2O, pH 10.3, 32 μl) was added and the incubation was continued for 2 h. The solution was dialyzed in 50 mM AcONa + 150 mM NaCl (pH 5.0) at 4 °C for 24 h and then purified on a gel filtration column (Superdex 200 HiLoad 16/60) using the BioLogic DuoFlow chromatography system (Bio-Rad) equipped with an analytical UV flow cell. The purification was done in 50 mM AcONa + 150 mM NaCl (pH 5.0) at a flow rate of 1 ml/min (fraction size = 0.5 ml from 56 to 80 min). The course of the purification was monitored by UV at 280 nm, and fractions between 59 and 70 ml (see chromatogram in Fig. 1) were combined, concentrated, dialyzed in phosphate-buffered saline (PBS, pH 7.4), and analyzed by FT–IR to quantify the concentration of Fp entities, thereby leading to the dendrimer concentration. Absorbance measurement at 280 nm afforded the IgG concentration (A_{280} = 1.4 for 1 mg/ml solution) after subtraction of the contribution of the dendrimer obtained from the previously established calibration curve $A_{280} = f$[dendrimer].

Immunoreactivity of the antibody–dendrimer conjugates

Binding of antibody–dendrimer conjugates to rabbit IgG-coated microplates was compared with binding of unmodified goat anti-rabbit IgG in the following manner. A rabbit IgG solution (100 μl/well, 5 μg/ml, in PBS, pH 7.4) was pipetted in a 96-well microtiter

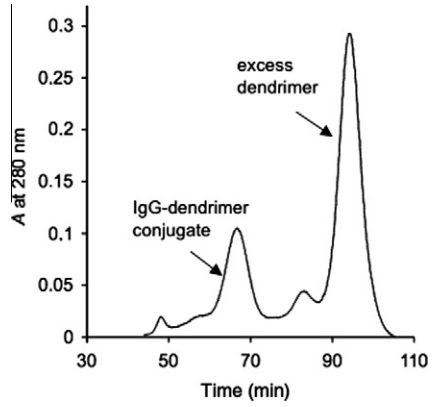

Fig.1. Chromatographic profile obtained for the purification of IgG–dendrimer conjugate from excess dendrimer with a Superdex 200 HiLoad column at a flow rate of 1 ml/min.

plate (F-bottom, Greiner) and left overnight at 4 °C. Nonspecific binding was further blocked by PBS + 4% goat serum (200 μl/well). Goat anti-rabbit IgG or antibody–dendrimer conjugate dilutions ranging from 0.23 to 120 μg/ml were prepared in 50 mM citrate + 130 mM NaCl (pH 5.0, citrate buffer) with 2% goat serum, applied to the wells in duplicate (100 μl/well), and incubated for 2 h at room temperature in the dark. Wells were washed four times with citrate buffer + 0.05% Tween 20, and then goat anti-rabbit IgG–horseradish peroxidase (HRP) conjugate diluted 1:8000 in citrate buffer + 2% goat serum was applied to the wells (100 μl/well) for 2 h at room temperature in the dark. Wells were washed as above, and a 0.7-mg/ml solution of *o*-phenylenediamine in citrate–phosphate buffer (pH 5.0) + 0.012% (v/v) H_2O_2 was applied to the wells (100 μl/well). The color was developed for 10 min, and the enzymatic reaction was stopped by the addition of 2.5 M H_2SO_4 (50 μl/well). The absorbance was read at 490 nm with a microtiter plate reader (model 550, Bio-Rad).

Quantification of rabbit IgG on nitrocellulose membrane by CMIA

Rabbit IgG solutions (0.2–40 μg IgG) were spotted onto punched nitrocellulose disks (6 mm diameter) with the amount of β-lactoglobulin (β-LG) solution (prepared at 10 mg/ml) necessary to coat each membrane with the same total amount of protein (40 μg). Two other membranes were coated with β-LG (40 μg): one to provide a reference IR spectrum (reference) and the other to measure nonspecific interactions (blank). Membranes were air-dried for 1 h and then incubated with blocking buffer (NaPB + 4% skimmed milk) for 90 min at room temperature. Membranes were washed two times with citrate buffer + 1.25% skimmed milk (0.8 ml/membrane in microtube with stirring). Each membrane was then incubated for 2 h at room temperature in the dark with Fp-labeled goat anti-rabbit IgG (0.3 nmol) in diluted blocking buffer (citrate buffer [pH 6.0] + 2% skimmed milk, 150 μl) except for the reference membrane, which was incubated without antibody. Membranes were washed five times with citrate buffer + 1.25% skimmed milk (0.8 ml/membrane in microtube with stirring) and air-dried for at least 2 h before IR analysis. Absorbances at 2052 cm^{-1} were corrected by measurements taken from the blank.

Results and discussion

A new synthetic route to homogeneous hydrazide-based Fp-labeled G4–PAMAM dendrimer

The first functionalization step of G4–PAMAM dendrimer consisted in the combined introduction of the hydrazide-terminated spacer arm (*N*-Boc protected) and the nitroaromatic NMR probe. For this purpose, compound **1** was first prepared independently by acylation of the aminohydrazide spacer with the activated ester of 4-fluoro-3-nitrobenzoic acid (Scheme 1, Eq. A) and was allowed to react with the dendrimer (Scheme 1, Eq. B). Labeling with Fp–maleimide, acetylation of the remaining accessible primary amino groups of the dendrimer and cleavage of the *N*-Boc protective group were then carried out according to established procedures [50]. This new synthetic route brought several advantages compared with the previous one [50]: (i) it reduced the number of steps from five to four; (ii) it prevented polymerization or aggregation observed when the acylation of the aminohydrazide spacer was carried out on the dendrimer, leading to an overall yield twice as high as that first reported; and (iii) it brought functional homogeneity on the dendrimer surface because all of the nitroaromatic residues now carry the hydrazide-terminated spacer brought by compound **1**.

Coupling of the hydrazide-based Fp-labeled G4–PAMAM dendrimer to goat anti-rabbit IgG and characterization of IgG–dendrimer conjugates

The conjugation procedure was based on the orthogonal ligation between aldehyde groups of goat anti-rabbit IgG generated by mild oxidation of the carbohydrate moieties [44,53] and hydrazide residues of the dendrimers (Scheme 2). After stabilization of the hydrazone linkage by reduction with $NaBH_3CN$ and the addition of ethanolamine to block the remaining free aldehyde groups [5], the immunoconjugate was isolated from excess dendrimer using size exclusion gel chromatography (Fig. 1).

To evaluate the average number of dendrimers conjugated per IgG, concentrations of both IgG and dendrimer in the conjugate solutions were then estimated by combining UV and FT–IR spectroscopies. First, the concentration of Fp labels was quantified by FT–IR. Solutions in PBS were spotted on nitrocellulose membranes, and then dried membranes were analyzed (Fig. 2A). The 2052-cm^{-1} peak height was measured and then related to the concentration of Fp units using the calibration curve established from standard solutions of Fp–maleimide in the range of 50 to 660 nmol/ml (Fig. 2B). This concentration gave access to the estimated concentration of the dendrimer knowing the average number of Fp units attached per dendrimer determined independently by NMR measurements [50]. On the other hand, for each dendrimer solution ready for antibody coupling, a UV calibration curve was established by plotting the absorbance at 280 nm (A_{280}) versus dendrimer concentration in the range of 0.625 to 20 nmol/ml. This calibration curve allowed us to determine the contribution of the dendrimer absorption at 280 nm in the conjugate solution knowing its concentration from FT–IR quantification. Then A_{280} of the IgG in the conjugate solution was easily determined as the difference between total A_{280} of the conjugate solution and A_{280} of the dendrimer (ε_{IgG} = 210,000 mol^{-1} cm^{-1}).

Two conjugates were also analyzed by MALDI–TOF mass spectrometry using a dedicated high-mass detection system (HM1) allowing enhanced sensitivity in the high-mass range and avoiding detector saturation due to intense low-mass species (e.g., matrix) [52,54]. Fig. 3 shows the mass spectra of the underivatized IgG (panel A) and two antibody–dendrimer conjugates with conjugation rates of 0.5 for conjugate 1 (panel B) and 1.2 for conjugate 2 (panel C) as estimated by UV and FT–IR measurements. Figs. 3B and 3C display broad peaks around *m*/*z* 168,000, corresponding to the antibody labeled with 1 dendrimer. Peaks are broadened, as is usually observed with PAMAM dendrimers higher than generation 3 [50,55–57], and this feature is retained even when conjugated to a protein. Underivatized IgG was present in a large amount in conjugate 1 (Fig. 3B), consistent with the estimation of 0.5 dendrimer per IgG determined by combining UV and FT–IR quantification.

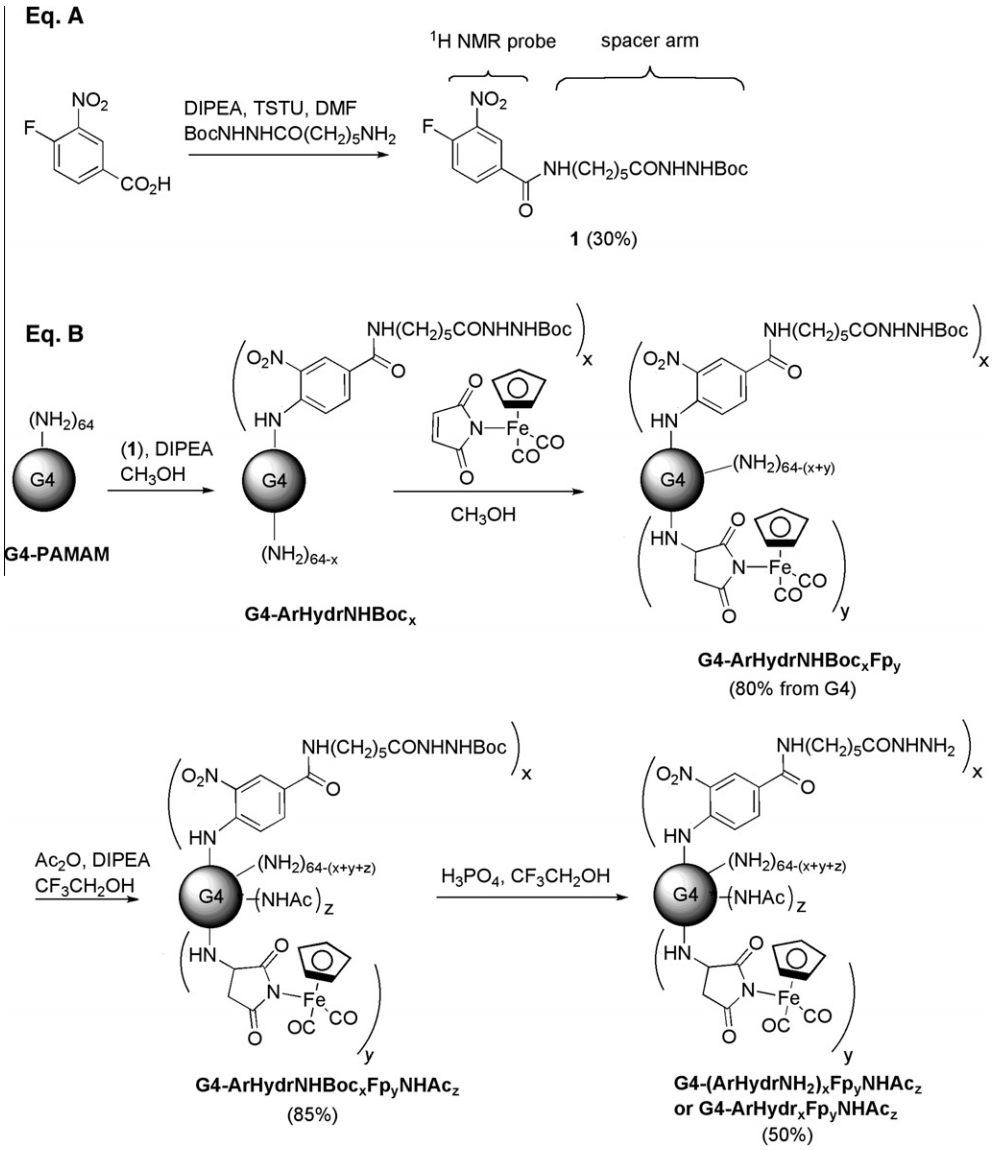

Scheme 1. Improved synthetic route to the hydrazide-based trifunctional G4–PAMAM dendrimer.

Conversely, nearly all of the IgG molecules appear to be derivatized in conjugate 2, also consistent with the estimation of 1.2 dendrimers per IgG determined by UV and FT–IR quantification. Moreover, in this latter conjugate, a peak around *m*/*z* 183,000 can be assigned to the antibody labeled with two dendrimers. Our method combining UV and FT–IR measurements to estimate the average number of dendrimers attached per antibody is in agreement with the distribution patterns obtained by MALDI–TOF mass spectrometry.

To optimize the multilabeling of the antibody, we studied the influence of pH, temperature, and reaction time on the conjugation reaction. First, Table 1 shows the number of dendrimers linked per antibody when the conjugation was carried out in acetate buffer at pH 6.5 or 5.1. Results clearly show that lowering the pH of the reaction buffer has a positive effect on the coupling rate regardless of the average number of Fp units attached to the dendrimer. Second, with the conjugation reaction being fixed at pH 5.1, the effect of temperature was studied. With a dendrimer carrying 28 Fp units, an average conjugation ratio of 0.6 dendrimer per antibody was obtained when the macromolecules were reacted for 4 h at room temperature, and then for 14 h at 4 °C, versus 1.0 dendrimer per antibody when the reaction mixture was left for 18 h at room temperature, indicating that the reaction was slow.

Experimental conditions being fixed at pH 5.1 and room temperature for 18 h, Table 2 shows the number of dendrimers linked per antibody starting from two dendrimer samples carrying 28 and 22 Fp units (i.e., an average of 25 Fp units). Average coupling ratios of 1.0 and 1.5, respectively, were obtained, indicating a positive effect of the spacer given that we previously reported a conjugation ratio of 0.5 with a dendrimer without spacer carrying 25 Fp units [44]. Regarding the average number of Fp probes linked per antibody, we were able to prepare immunoconjugates with averages of 33 and 28 Fp probes with $G4(ArHydr)_4Fp_{22}NHAc_{21}$ and $G4(ArHydr)_5Fp_{28}NHAc_{18}$, respectively. An average of 30 Fp probes per antibody represents more than twice the number of 13 previously reported without the spacer. This result clearly shows that the newly engineered dendrimer significantly improved the loading in IR probes of the immunoconjugates.

Immunoreactivity

The immunoreactivity of the antibody–dendrimer conjugates was then determined by a two-step immunoassay with microplates coated with rabbit IgG. The first incubation step was performed by the addition of standard solutions of commercial

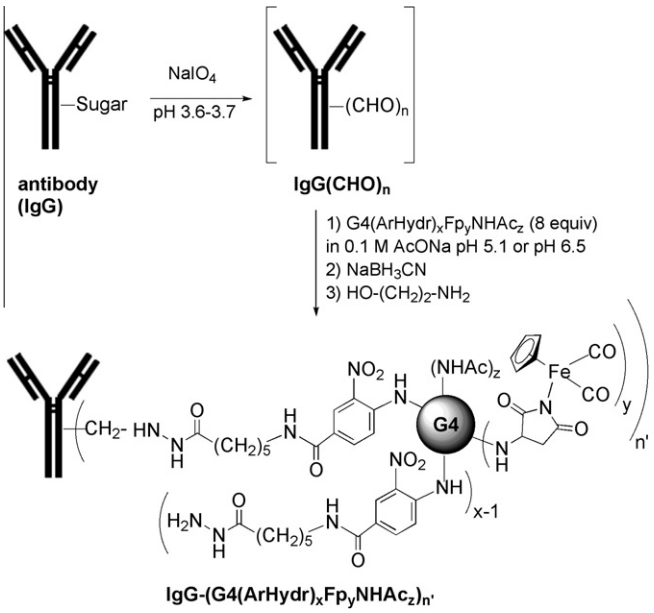

Scheme 2. Synthetic route to IgG–dendrimer conjugates.

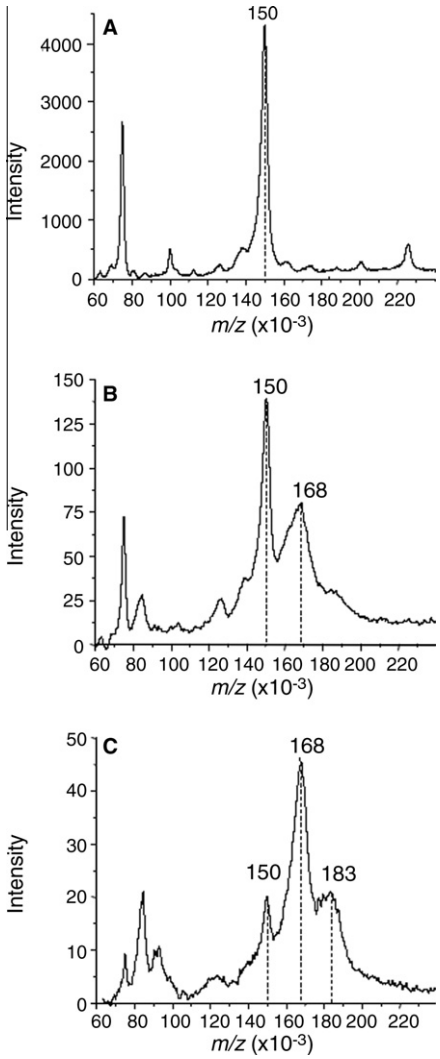

Fig.3. High-mass MALDI–TOF mass spectrometry for underivatized IgG (A), IgG–$[G4(ArHydr)_4Fp_{29}NHAc_{14}]_{0.5}$ (B), and IgG–$[G4(ArHydr)_4Fp_{22}NHAc_{21}]_{1.2}$ (C).

(underivatized) or dendrimer-conjugated goat anti-rabbit IgG. Peroxidase-conjugated goat anti-rabbit IgG was incubated in a second step, and the immunoreactivities relative to the commercial IgG were calculated from the corresponding IC_{50} values. An assay was performed with the dendrimer alone to assess the level of nonspecific interaction between the dendrimer and the sensitized plate and/or between the dendrimer and the secondary antibody. The working concentrations in the assay were equal to those of the dendrimer in the conjugate samples taking into account the conjugation rate. It was shown that running the assay in classical PBS buffer at pH 7.4 led to nonspecific interactions (the engineered dendrimer tends to stick to the protein coated to the plate, leading to the formation of a sandwich coated protein/dendrimer/secondary antibody, presumably owing to electrostatic interactions), whereas running the assay at pH 5.0 in citrate buffer eliminated nonspecific interactions at the working concentrations used. Consequently, all of the assays were performed at pH 5.0 in citrate buffer. The immunoreactivity of the antibody–dendrimer conjugates was found to be between 41.4 and 66.2% of that of the underivatized antibody depending on the degree of antibody derivatization (Table 3), with an average immunoreactivity of 55.1%. A high labeling decreased the immunoreactivity, as evidenced by entry 5 in Table 3, although the conjugation strategy was site selective to

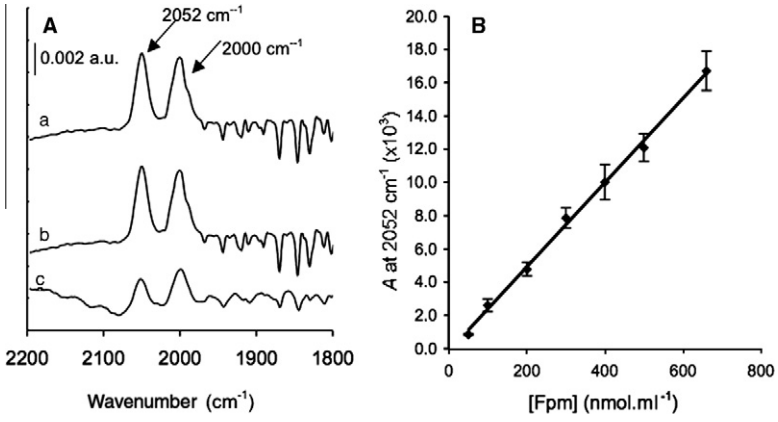

Fig.2. Quantification of Fp labels by FT–IR spectroscopy on nitrocellulose membranes. (A) Here 4 μl of the following solutions was deposited and left to dry: IgG–$[G4(ArHydr)4Fp_{29}NHAc_{14}]_{0.6}$, 5.4 nmol/ml (a); IgG–$[G4(ArHydr)_4Fp_{22}NHAc_{21}]_{1.3}$, 11.8 nmol/ml (b); IgG–$[G4(ArHydr)_3Fp_{26}NHAc_9]_{1.3}$, 5.7 nmol/ml (c). The 2052 cm^{-1} "analytical peak" height is proportional to the concentration of the Fp complex. a.u., arbitrary units. (B) Calibration curve of Fp–maleimide (Fpm) in the range of 50 to 660 nmol/ml.

Table 1
Number of dendrimers linked per antibody when the conjugation was carried out at pH 6.5 or 5.1.

Dendrimer	pH 6.5	pH 5.1
$G4(ArHydr)_4Fp_{29}NHAc_{14}$	0.6 ± 0.2	1.0 ± 0.2
$G4(ArHydr)_4Fp_{22}NHAc_{21}$	1.0 ± 0.2	1.3 ± 0.2

Note. Values are means ± standard deviations ($n = 2$).

Table 2
Number of dendrimers and Fp probes attached per antibody molecule depending on the synthetic strategy followed for the preparation of the dendrimer.

Dendrimer	Number of dendrimers per antibody	Number of Fp probes per antibody
$G4(ArHydr)_5Fp_{28}NHAc_{18}$	1.0 ± 0.2	28 ± 7
$G4(ArHydr)_4Fp_{22}NHAc_{21}$	1.5 ± 0.2	33 ± 5
$G4(Fp_{25})$ [44]	0.5 ± 0.1	13 ± 2

Note. Values are means ± standard deviations ($n = 3$).

Table 3
Immunoreactivity of the antibody–dendrimer conjugates relative to the immunoreactivity of the underivatized antibody.

Entry	Antibody–dendrimer conjugate	Immunoreactivity retained (%)
1	$IgG–[G4(ArHydr)_5Fp_{28}NHAc_{18}]_{0.6}$	66.2
2	$IgG–[G4(ArHydr)_5Fp_{28}NHAc_{18}]_{0.8}$	60.0
3	$IgG–[G4(ArHydr)_4Fp_{22}NHAc_{21}]_1$	52.9
4	$IgG–[G4(ArHydr)_5Fp_{29}NHAc_{14}]_1$	55.8
5	$IgG–[G4(ArHydr)_4Fp_{22}NHAc_{21}]_{1.8}$	41.4

the Fc region of the IgG and thereby remote from the antibody–antigen binding site. On the other hand, the number of bulky metal carbonyl complexes carried by the dendrimer did not influence the immunoreactivity, as exemplified by entries 3 and 4 in Table 3. Antibody–dendrimer conjugates preserved good immunoreactivity provided that the conjugation ratio was not too high, which seems to favor a high dendrimer loading over a high antibody–dendrimer conjugation ratio.

Quantification of rabbit IgG by CMIA

In a second experiment, we then studied the ability of these new IgG–dendrimer conjugates to quantify their related antigen, namely rabbit IgG, by CMIA on nitrocellulose membrane. In fact, this test corresponds to the second step in classical immunoassays, the interaction between primary and secondary antibodies, with secondary antibodies commonly labeled with enzyme, fluorescent compound, or biotin as detectable probes. Here secondary antibodies were labeled with IR probes (Scheme 3). Rabbit IgG in the range of 0.2 to 40 μg (1.3–266.7 pmol) was spotted onto membranes with concomitant quantities of β-LG, which is not recognized by goat anti-rabbit IgG, so that the total amount of protein adsorbed per membrane remained the same (40 μg). Membranes were air-dried and blocked with 4% dried skimmed milk. Each membrane was then incubated with 0.3 nmol of goat anti-rabbit IgG–dendrimer conjugate ($IgG–[G4(ArHydr)_4Fp_{22}NHAc_{21}]_{1.3}$) in citrate buffer (pH 6.0), washed, dried, and analyzed by IR in the transmission mode. Curve a in Fig. 4 shows the absorbance of the 2052-cm^{-1} band versus the amount of rabbit IgG on the membrane. For a given amount of antigen on the membrane, a higher absorbance was measured compared with results obtained with the first generation of Fp-labeled IgG–dendrimer conjugate ($IgG–[G4(Fp_{10})_{1.4}]$) (Fig. 4, curve b). For instance, an absorbance of 7.8 x 10^{-3} was measured for the membrane coated with 10 μg (66.7 pmol) of rabbit IgG instead of 3.3 x 10^{-3} using the first conjugate generation. Moreover, this result was obtained with a lower amount of labeled antibody in the assay (0.3 vs. 0.8 nmol). This experiment clearly shows the efficiency of the new multilabeling procedure given that the IR signal was more than twice as high, although 2.7 times less labeled antibody was employed in the assay.

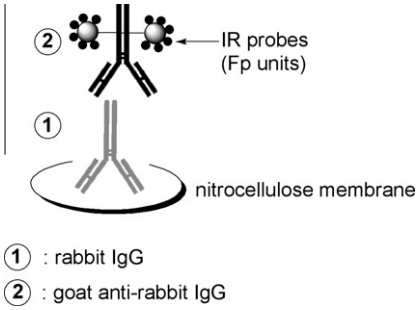

Scheme 3. Schematic interaction between rabbit IgG (primary antibody) and goat anti-rabbit IgG–dendrimer conjugate (secondary antibody) at the surface of nitrocellulose membranes. IR probes located on the IgG–dendrimer conjugate allow the quantification of rabbit IgG by FT–IR (see Fig. 4).

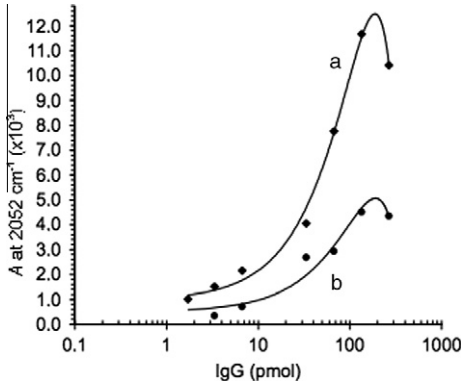

Fig.4. Quantification of rabbit IgG on nitrocellulose membranes by using an excess of Fp-labeled goat anti-rabbit IgG with 0.3 nmol per assay of Fp-labeled antibody–dendrimer conjugate with spacer arm (sample $IgG–[G4(ArHydr)_4Fp_{22}NHAc_{21}]_{1.3}$) (a) and with 0.8 nmol per assay of Fp-labeled antibody–dendrimer conjugate without spacer arm (sample $IgG–[G4(Fp_{10})_{1.4}]$) (b) [44].

Conclusion

We have described the site-directed conjugation of hydrazide-based G4–PAMAM dendrimers carrying 22 to 29 organometallic Fp labels on average to the oxidized glycosylated part of an antibody. First an improved synthetic route to the labeled dendrimers was reported, and then the bioconjugation conditions were optimized so as to reach an average coupling ratio of 1 dendrimer per IgG with a dendrimer carrying 28 Fp labels or 1.5 dendrimers per IgG with a dendrimer carrying 22 Fp labels. At the organometallic probe level, we were able to prepare immunoconjugates with 30 Fp units on average, which is more than twice the value previously reported without the spacer. Thus, the newly designed Fp-labeled dendrimer proved to be more efficient for the multilabeling of aldehyde-containing molecules with metal carbonyl probes. These antibody–dendrimer conjugates were characterized by combining UV and FT–IR measurements. High-mass MALDI–TOF mass spectrometry experiments confirmed the covalent coupling as well as the estimated conjugation ratio. For the first time, immunoreactivity studies were conducted and revealed that our antibody–

metallodendrimer conjugates retained an average of 55.1% of that of the underivatized antibody. Finally, these conjugates were evaluated as a universal detection reagent for the solid-phase CMIA quantification of rabbit IgG on nitrocellulose membrane. Significantly enhanced intensities of the IR detection signal were observed, confirming the efficiency of the new bioconjugation strategy. The next step will be the development of a full solid-phase immunoassay with primary and then secondary antigen–antibody interactions for the quantification of relevant analytes.

Acknowledgments

The Centre National de la Recherche Scientifique and the French Ministry of Research are gratefully acknowledged for financial support.

References

[1] D.A. Tomalia, H. Baker, J.R. Dewald, M. Hall, G. Kallos, S. Martin, J. Roeck, J. Ryder, P. Smith, A new class of polymers: Starburst-dendritic macromolecules, Polym. J. 17 (1985) 117–132.
[2] D.A. Tomalia, H. Baker, J.R. Dewald, M. Hall, G. Kallos, S. Martin, J. Roeck, J. Ryder, P. Smith, Dendritic macromolecules: synthesis of Starburst dendrimers, Macromolecules 19 (1986) 2466–2468.
[3] D.A. Tomalia, A.M. Naylor, W.A. Goddard III, Starburst dendrimers: molecular-level control of size, shape, surface chemistry, topology, and flexibility from atoms to macroscopic matter, Angew. Chem. Int. Ed. 29 (1990) 138–175.
[4] D.A. Tomalia, Birth of a new macromolecular architecture: dendrimers as quantized building blocks for nanoscale synthetic polymer chemistry, Prog. Polym. Sci. 30 (2005) 294–324.
[5] G.T. Hermanson, Bioconjugate Techniques, Academic Press, San Diego, 2008.
[6] A.R. Menjoge, R.M. Kannan, D.A. Tomalia, Dendrimer-based drug and imaging conjugates: design considerations for nanomedical applications, Drug Discovery Today 15 (2010) 171–185.
[7] I.J. Majoros, C.R. Williams, J.R. Baker, Current dendrimer applications in cancer diagnosis and therapy, Curr. Top. Med. Chem. 8 (2008) 1165–1179.
[8] S. Svenson, Dendrimers as versatile platform in drug delivery applications, Eur. J. Pharm. Biopharm. 71 (2009) 445–462.
[9] S.H. Medina, M.E.H. El-Sayed, Dendrimers as carriers for delivery of chemotherapeutic agents, Chem. Rev. 109 (2009) 3141–3157.
[10] C.M. Paleos, D. Tsiourvas, Z. Sideratou, Molecular engineering of dendritic polymers and their application as drug and gene delivery systems, Mol. Pharm. 4 (2007) 169–188.
[11] N.K. Jain, A. Asthana, Dendritic systems in drug delivery applications, Expert Opin. Drug Deliv. 4 (2007) 495–512.
[12] S. Bai, C. Thomas, A. Rawat, F. Ahsan, Recent progress in dendrimer-based nanocarriers, Crit. Rev. Ther. Drug Carrier Syst. 23 (2006) 437–495.
[13] U. Boas, P.M.H. Heegaard, Dendrimers in drug research, Chem. Soc. Rev. 33 (2004) 43–63.
[14] Y. Cheng, Z. Xu, M. Ma, T. Xu, Dendrimers as drug carriers: applications in different routes of drug administration, J. Pharm. Sci. 97 (2008) 123–143.
[15] R. Esfand, D.A. Tomalia, Poly(amidoamine) (PAMAM) dendrimers: from biomimicry to drug delivery and biomedical applications, Drug Discovery Today 6 (2001) 427–436.
[16] E.R. Gillies, J.M.J. Fréchet, Dendrimers and dendritic polymers in drug delivery, Drug Discovery Today 10 (2005) 35–43.
[17] A.K. Patri, I.J. Majoros, J.R. Baker Jr., Dendritic polymer macromolecular carriers for drug delivery, Curr. Opin. Chem. Biol. 6 (2002) 466–471.
[18] S. Svenson, D.A. Tomalia, Dendrimers in biomedical applications: reflections on the field, Adv. Drug Deliv. Rev. 57 (2005) 2106–2129.
[19] V.J. Venditto, C.A.S. Regino, M.W. Brechbiel, PAMAM dendrimer based macromolecules as improved contrast agents, Mol. Pharm. 2 (2005) 302–311.
[20] H. Kobayashi, M.W. Brechbiel, Nano-sized MRI contrast agents with dendrimer cores, Adv. Drug Deliv. Rev. 57 (2005) 2271–2286.
[21] S-E. Stiriba, H. Frey, R. Haag, Dendritic polymers in biomedical applications: from potential to clinical use in diagnostics and therapy, Angew. Chem. Int. Ed. 41 (2002) 1329–1334.
[22] H. Xu, C.A.S. Regino, Y. Koyama, Y. Hama, A.J. Gunn, M. Bernardo, H. Kobayashi, P.L. Choyke, M.W. Brechbiel, Preparation and preliminary evaluation of a biotin-targeted, lectin-targeted dendrimer-based probe for dual-modality magnetic resonance and fluorescence imaging, Bioconjugate Chem. 18 (2007) 1474–1482.
[23] C. Wängler, G. Moldenhauer, R. Saffrich, E-M. Knapp, B. Beijer, M. Schnölzer, B. Wängler, M. Eisenhut, U. Haberkorn, W. Mier, PAMAM structure-based multifunctional fluorescent conjugates for improved fluorescent labeling of biomacromolecules, Chem. Eur. J. 14 (2008) 8116–8130.
[24] L. Svobodova, M. Snejdarkova, V. Polohova, I. Grman, P. Rybar, T. Hianik, QCM immunosensor based on polyamidoamine dendrimers, Electroanalysis 18 (2006) 1943–1949.
[25] M. Snejdarkova, L. Svobodova, G. Evtugyn, H. Budnikov, A. Karyakin, D.P. Nikolelis, T. Hianik, Acetylcholinesterase sensors based on gold electrodes modified with dendrimer and polyaniline: a comparative research, Anal. Chim. Acta 514 (2004) 79–88.
[26] L. Svobodova, M. Snejdarkova, T. Hianik, Properties of glucose biosensors based on dendrimer layers: effect of enzyme immobilization, Anal. Bioanal. Chem. 373 (2002) 735–741.
[27] H.C. Yoon, D. Lee, H-S. Kim, Reversible affinity interactions of antibody molecules at functionalized dendrimer monolayer: affinity-sensing surface with reusability, Anal. Chim. Acta 456 (2002) 209–218.
[28] H-J. Seok, M-Y. Hong, Y-J. Kim, M-K. Han, D. Lee, J-H. Lee, J-S. Yoo, H-S. Kim, Mass spectrometric analysis of affinity-captured proteins on a dendrimer-based immunosensing surface: investigation of on-chip proteolytic digestion, Anal. Biochem. 337 (2005) 294–307.
[29] M.A. Rahman, H-B. Noh, Y-B. Shim, Direct electrochemistry of laccase immobilized on Au nanoparticles encapsulated–dendrimer bonded conducting polymer: application for a catechin sensor, Anal. Chem. 80 (2008) 8020–8027.
[30] P. Singh, Dendrimers and their applications in immunoassays and clinical diagnostics, Biotechnol. Appl. Biochem. 48 (2007) 1–9.
[31] K.K. Ong, A.L. Jenkins, R. Cheng, D.A. Tomalia, H.D. Durst, J.L. Jensen, P.A. Emanuel, C.R. Swim, R. Yin, Dendrimer enhanced immunosensors for biological detection, Anal. Chim. Acta 444 (2001) 143–148.
[32] M. Zhou, J. Roovers, G.P. Robertson, C.P. Grover, Multilabeling biomolecules at a single site: 1. Synthesis and characterization of a dendritic label for electrochemiluminescence assays, Anal. Chem. 75 (2003) 6708–6717.
[33] C. Wu, M.W. Brechbiel, R.W. Kozak, O.A. Gansow, Metal–chelate–dendrimer–antibody constructs for use in radioimmunotherapy and imaging, Bioorg. Med. Chem. Lett. 4 (1994) 449–454.
[34] H. Kobayashi, C. Wu, M-K. Kim, C.H. Paik, J.A. Carrasquillo, M.W. Brechbiel, Evaluation of the in vivo biodistribution of indium-111 and yttrium-88 labeled dendrimer–1B4M–DTPA and its conjugation with anti-Tac monoclonal antibody, Bioconjugate Chem. 10 (1999) 103–111.
[35] A.K. Patri, A. Myc, J. Beals, T.P. Thomas, N.H. Bander, J.R. Baker Jr., Synthesis and in vitro testing of J591 antibody–dendrimer conjugates for targeted prostate cancer therapy, Bioconjugate Chem. 15 (2004) 1174–1181.
[36] T.P. Thomas, A.K. Patri, A. Myc, M.T. Myaing, J.Y. Ye, T.B. Norris, J.R. Baker Jr., In vitro targeting of synthesized antibody-conjugated dendrimer nanoparticles, Biomacromolecules 5 (2004) 2269–2274.
[37] R. Shukla, T.P. Thomas, J.L. Peters, A.M. Desai, J. Kukowska-Latallo, A.K. Patri, A. Kotlyar, J.R. Baker Jr., HER2 specific tumor targeting with dendrimer conjugated anti-HER2 mAb, Bioconjugate Chem. 17 (2006) 1109–1115.
[38] C. Wängler, G. Moldenhauer, M. Eisenhut, U. Haberkorn, W. Mier, Antibody–dendrimer conjugates: the number, not the size of the dendrimers, determines the immunoreactivity, Bioconjugate Chem. 19 (2008) 813–820.
[39] R.F. Barth, D.M. Adams, A.H. Soloway, F. Alam, M.V. Darby, Boronated Starburst dendrimer–monoclonal antibody immunoconjugates: evaluation as a potential delivery system for neutron capture therapy, Bioconjugate Chem. 5 (1994) 58–66.
[40] R. Shukla, T.P. Thomas, A.M. Desai, A. Kotlyar, S.J. Park, J.R. Baker Jr., HER2 specific delivery of methotrexate by dendrimer conjugated anti-HER2 mAb, Nanotechnology 19 (2008) 295102–295108.
[41] J.C. Roberts, Y.E. Adams, D.A. Tomalia, J.A. Mercer-Smith, D.K. Lavallee, Using Starburst dendrimers as linker molecules to radiolabel antibodies, Bioconjugate Chem. 1 (1990) 305–308.
[42] L.P. Tolic, G.A. Anderson, R.D. Smith, H.M. Brothers II, R. Spindler, D.A. Tomalia, Electrospray ionization Fourier transform ion cyclotron resonance mass spectrometric characterization of high molecular mass Starburst dendrimers, Int. J. Mass Spectrom. Ion Processes 165-166 (1997) 405–418.
[43] G. Wu, R.F. Barth, W. Yang, M. Chatterjee, W. Tjarks, M.J. Ciesielski, R.A. Fenstermaker, Site-specific conjugation of boron-containing dendrimers to anti-EGF receptor monoclonal antibody Cetuximab (IMB-C225) and its evaluation as a potential delivery agent for neutron capture therapy, Bioconjugate Chem. 15 (2004) 185–194.
[44] N. Fischer-Durand, M. Salmain, B. Rudolf, A. Vessières, J. Zakrzewski, G. Jaouen, Synthesis of metal–carbonyl–dendrimer–antibody immunoconjugates: towards a new format for carbonyl metallo immunoassay, ChemBioChem 5 (2004) 519–525.
[45] M. Salmain, A. Vessières, G. Jaouen, I.S. Butler, Fourier transform infrared spectroscopic method for the quantitative trace analysis of transition-metal carbonyl-labeled bioligands, Anal. Chem. 63 (1991) 2323–2329.
[46] M. Salmain, A. Vessières, P. Brossier, I.S. Butler, G. Jaouen, Carbonylmetalloimmunoassay (CMIA), a new type of non-radioisotopic immunoassay: Principles and application to phenobarbital assay, J. Immunol. Methods 148 (1992) 65–75.
[47] A. Vessières, M. Salmain, P. Brossier, G. Jaouen, Carbonyl metallo immunoassay: a new application for Fourier transform infrared spectroscopy, J. Pharm. Biomed. Anal. 21 (1999) 625–633.
[48] A. Vessières, F. Le Bideau, N. Fischer-Durand, P. Janvier, J-M. Heldt, S. Ben Rejeb, G. Jaouen, First carbonyl metallo immunoassay (CMIA) in the environmental area: application to the herbicide chlortoluron, Appl. Organomet. Chem. 16 (2002) 669–674.
[49] M. Salmain, A. Vessières, Organometallic complexes as tracers in non-isotopic immunoassay, in: G. Jaouen (Ed.), Bioorganometallics, Biomolecules, Labeling, Medicine, Wiley–VCH, Weinheim, Germany, 2006, pp. 263–302.
[50] N. Fischer-Durand, M. Salmain, B. Rudolf, L. Jugé, V. Guérineau, O. Laprévote, A. Vessières, G. Jaouen, Design of a new multifunctionalized PAMAM dendrimer with hydrazide-terminated spacer arm suitable for metal–carbonyl

multilabeling of aldehyde-containing molecules, Macromolecules 40 (2007) 8568–8575.
[51] B. Rudolf, J. Zakrzewski, (η^5-Cyclopentadienyl)Fe(CO)$_2$ complex of maleimide anion: an organometallic carbonyl probe for biomolecules containing HS groups, Tetrahedron Lett. 35 (1994) 9611.
[52] U. Bahr, U. Rohling, C. Lautz, K. Strupat, M. Schurenberg, F. Hillenkamp, A charge detector for time-of-flight mass analysis of high mass ions produced by matrix-assisted laser desorption/ionisation (MALDI), Int. J. Mass Spectrom. Ion Processes 153 (1996) 9–21.
[53] C.A.C. Wolfe, D.S. Hage, Studies on the rate and control of antibody oxidation by periodate, Anal. Biochem. 231 (1995) 123–130.
[54] T. Pimenova, C.P. Pereira, D.J. Schaer, R. Zenobi, Characterization of high molecular weight multimeric states of human haptoglobin and hemoglobin-based oxygen carriers by high-mass MALDI MS, J. Sep. Sci. 32 (2009) 1224–1230.
[55] E.K. Woller, E.D. Walter, J.R. Morgan, D.J. Singel, M.J. Cloninger, Altering the strength of lectin binding interactions and controlling the amount of lectin clustering using mannose/hydroxyl-functionalized dendrimers, J. Am. Chem. Soc. 125 (2003) 8820–8826.
[56] M-Y. Hong, Y-J. Kim, J.W. Lee, K. Kim, J-H. Lee, J-S. Yoo, S-H. Bae, B-S. Choi, H-S. Kim, Synthesis and characterization of tri(ethylene oxide)-attached poly(amidoamine) dendrimer layer on gold, J. Colloid Interface Sci. 274 (2004) 41–48.
[57] E. Hill, R. Shukla, S.S. Park, J.R. Baker Jr., Synthetic PAMAM–RGD conjugates target and bind to odontoblast-like MDPC 23 cells and the predentin in tooth organ cultures, Bioconjugate Chem. 18 (2007) 1756–1762.